

05

Influence of microcracks on Poisson's ratio during plastic deformation of austenitic steel

© S.V. Kirikov, V.V. Mishakin, V.A. Klyushnikov

Mechanical Engineering Research Institute of RAS branch of Federal State Budgetary Scientific Institution "Federal Research Center The Institute of Applied Physics of the RAS",
603024 Nizhny Novgorod, Russia
e-mail: imndt31@mts-nn.ru

Received October 15, 2021

Revised December 7, 2021

Accepted December 8, 2021

We researched the influence of damage accumulation on the Poisson's ratio measured by echo-pulse acoustic method during plastic deformation of 12Kh18N10T steel. On the basis of the obtained experimental data we calculated the partial contributions to the change in the Poisson's ratio of damage accumulation and formation of the strain induced martensite phase. The characteristics of stable cracks forming near strain-induced martensite particles at small degrees of plastic strain have been analyzed by computer simulation. The theoretical dependence of the change in the Poisson's ratio due to crack formation during plastic deformation has been constructed. A good agreement between the experimental data and theoretical calculations has been obtained.

Keywords: plastic deformation, austenitic steel, Poisson's ratio, martensite transformation, dislocation, mesodefekt, configurational force method.

DOI: 10.21883/TP.2022.03.53262.277-21

Introduction

It is known, that plastic deformation of chromium-nickel steels with low stacking fault energy is accompanied with formation of a strain-induced martensite phase from initial austenite phase. Formation of the martensite phase with higher strength properties, compared to austenite phase, results in change of electromagnetic, elastic and acoustic properties of the whole material, and also influences the process of damage accumulation in softer austenite [1–5]. In [6] it is showed, that micro-cracks density has high correlation with volume fraction of the strain-induced martensite.

In the work [1] it is observed, that Poisson's ratio, defined using acoustic measurements, can be used as a diagnostic structural-sensitive parameter of austenite steel state at fatigue fracture. Poisson's ratio ν is expressed through the time or velocity of elastic waves the following way:

$$\nu = \frac{\tau_\tau^2 - 2\tau_l^2}{2(\tau_\tau^2 - \tau_l^2)} = \frac{V_l^2 - 2V_\tau^2}{2(V_l^2 - V_\tau^2)}, \quad (1)$$

where V_τ, V_l, t_τ, t_l are velocity and time of shear and longitudinal elastic waves respectively.

During deformation the Poisson's ratio ν is mainly influenced by two factors — accumulation of damage and formation of the strain-induced martensite phase:

$$\Delta\nu = \Delta\nu_\psi + \Delta\nu_\Phi, \quad (2)$$

where $\Delta\nu_\psi, \Delta\nu_\Phi$ are changes of the Poisson's ratio due to damage accumulation and formation of the strain-induced martensite phase respectively.

According to theoretical models, presented in the works [7–10], the formation and development of cracks result in reduction of elasticity modules and value of ν , while the formation of martensite — to increase of ν . Change of Poisson's ratio $\Delta\nu_\psi$ due to accumulation of damage ψ in the work [10] is defined the following way:

$$\Delta\nu_\psi = -\frac{3(1 - \nu_0^2)(5\nu_0 - 1)}{2(7 - 5\nu_0)} \psi, \quad (3)$$

where ν_0 is Poisson's ratio of undamaged material, $\psi = n_{cr} \bar{l}^3$, n_{cr} is cracks concentration, l is average cracks length.

Based on present electron microscopic studies [11], it is reasonable to assume that there are three characteristic stages of damage accumulation, related to formation of the strain-induced martensite phase in austenite steels at active plastic deformation:

- — at the first stage the volume fraction of martensite particles increases and micro-cracks density is accumulated near these particles;
- — the second stage is characterized with significant increase of density and length of micro-cracks, formed on particles of the strain-induced martensite;
- — at the third stage the loss of micro-crack stability happens and it transforms into the main crack.

At the first and seconds stages the density of stable cracks in internal stress fields increases due to mesodefekts [12–14], forming on particles of the strain-induced martensite during plastic deformation. As of now, the issue of model presentation for micro-damage (cracks) accumulation process, related to martensite particles formation, remains

open. Such model building and comparison of the results of theoretical calculations and results of experimental studies will give a fuller picture of fracture of metastable austenite steel under plastic deformation.

In this work the numerical modeling of characteristics of stable micro-cracks, forming on particles of the strain-induced martensite during plastic deformation, was performed based on experimental data and their influence on Poisson's ratio of austenite chromium-nickel steel 12Kh18N10T was studied.

1. Experimental technique

Studies of process of plastic deformation of steel 12Kh18N10T were performed using methods of ultrasound and eddy-current control. Chemical composition of the investigated steel (mass. %): C 0.02, Si 0.43, Mn 0.74, Cr 17.76, Ni 9.16, Ti 0.32, S 0.002, P 0.033, Cu 0.23, Fe basis.

Uniaxial elongation was performed with strain rate of 10^{-4} s^{-1} at room temperature. Length of a plane sample working part was 100 mm, width — 20 mm, thickness — 6 mm. Tests were performed at electromechanical multi-purpose pull test machine Tinius Olsen H100KU. Deformation was performed in stages, ultrasound and eddy-current studies were performed before the first stage (in initial state) and after each stage of loading until necking.

Elastic waves propagation time was measured using ultrasound echo-method. For excitation of shear and longitudinal waves the direct piezoelectric transducers V156 and V110 respectively, made by Olympus, with diameter of working plate of 6 mm and central frequency of 5 MHz were used. Longitudinal and shear waves propagated perpendicular to load axis. Polarization of shear waves were directed both along and across the load axis.

Ultrasonic flaw detector A1212 MASTER was used as electric pulses generator. Digital oscilloscope ADCLab was used for recording of the amplitude-time diagrams of echo-pulses, coming from piezoelectric transducers to a personal computer. Sampling frequency — 1 GHz, time resolution — 1 ns. As a result of data processing the time of propagation of elastic waves t_r and t_l after each loading stage was observed. During calculation of t_r the average value of propagation time of shear waves, polarized along and across the load axis, was used.

Propagation time measurement error was 2–3 ns, determination of Poisson's ratio — $7 \cdot 10^{-4}$.

Measurement of volume fraction of the strain-induced martensite phase Φ was performed using multi-purpose eddy-current device „MVP-2M“ after each loading stage. The device was pre-calibrated using samples with known martensite phase content. The relative measurement error did not exceed 5%.

2. Results of experimental studies

Eddy-current studies have showed the change of electromagnetic characteristics of 12Kh18N10T steel during plastic deformation. Dependence of volume fraction of the strain-induced martensite phase Φ on value of plastic strain ε_{pl} has a sigmoid form (Fig. 1, *a*), mathematical description of which was initially presented in the work [15].

As a result of acoustic studies the propagation time of shear and longitudinal elastic waves was defined and Poisson's ratio was calculated as per formula (1) (Fig. 1, *b*). It was observed, that at initial section of curve $\nu(\varepsilon_{pl})$ the rate of Poisson's ratio change $\Delta\nu/\Delta\varepsilon_{pl}$ is maximum. Increase of Poisson's ratio is related to a change of elasticity modules of the whole material, which are influenced by the strain-induced martensite particles formation. On a section of the developed plastic deformation the defects of dislocation type induce appearance of non-homogeneous fields of elastic stresses near these particles, provoking initiation and propagation of micro-cracks. Development of damage results in reduction of value of $\Delta\nu$, expression (3).

It is assumed, that on initial sections of deformation the dependence $\Delta\nu(\Phi)$ is linear (Fig. 1, *c*), and Poisson's ratio is defined with formation of magnetic phase only, then the change of $\Delta\nu_\Phi$, included in the expression (2), is the following

$$\Delta\nu_\Phi = k_\Phi \Delta\Phi, \quad (4)$$

where $k_\Phi = 0.0055$ (in formula (4) the volume fraction is expressed in fractions, while on figures — in percents).

Using the experimental data of Poisson's ratio change due to accumulation of damage $\Delta\nu_\psi^{(exp)}$ can be defined from expressions (2) and (4) as

$$\Delta\nu_\psi^{(exp)} = \Delta\nu - k_\Phi \Delta\Phi. \quad (5)$$

Figure 2 shows the change of Poisson's ratio ν and its components $\nu_\psi^{(exp)}$ and ν_Φ .

It was observed, that damage does not impact the Poisson's ratio ν_ψ at strain ε_{pl} , that do not exceed 5%. With the further deformation the martensite phase starts to separate more intensively (Fig. 1, *a*), impacting the component $\Delta\nu_\Phi$.

3. Modeling

Let's perform the theoretical study of Poisson's ratio change due to damage accumulation (cracks density). The assigned task we will solve in 2D-approximation (plane strain). Let's present the austenite matrix as an infinite elastic-isotropic continuous medium, that is characterized with shear modulus G and Poisson's ratio ν . The matrix contains isotropic particles of the second phase in the form of rectangles, of the same size with sides length of $2a_1$ and $2a_2$ ($a_1 \gg a_2$). Let's assume that distribution of these particles orientation as per angle of $\Omega \in [0, 2\pi)$ is isotropic (Fig. 3, *a*). Considering symmetry of deformation scheme

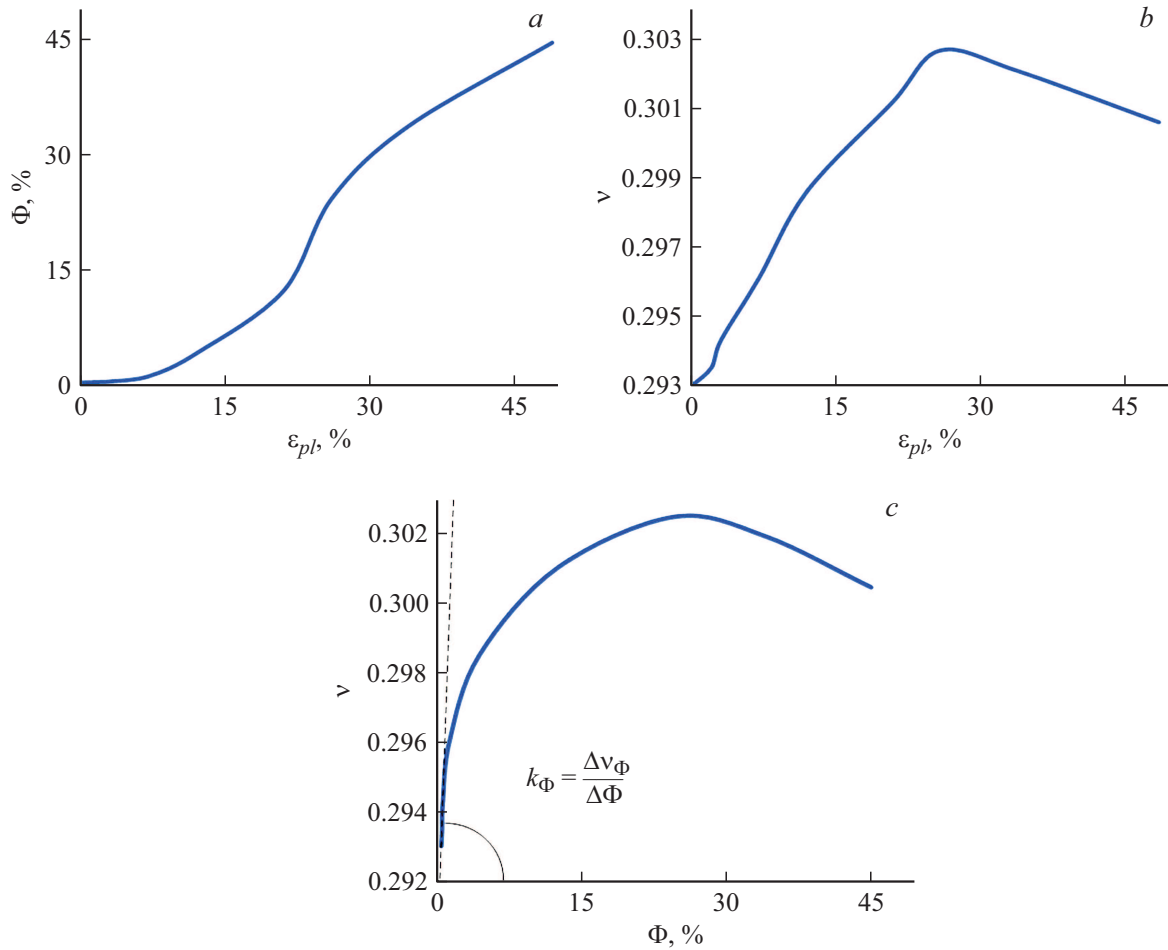


Figure 1. Dependencies of volume fraction of martensite phase Φ (a) and Poisson's ratio (b) on value of plastic deformation ε_{pl} , relation $\nu(\Phi)$ (c).

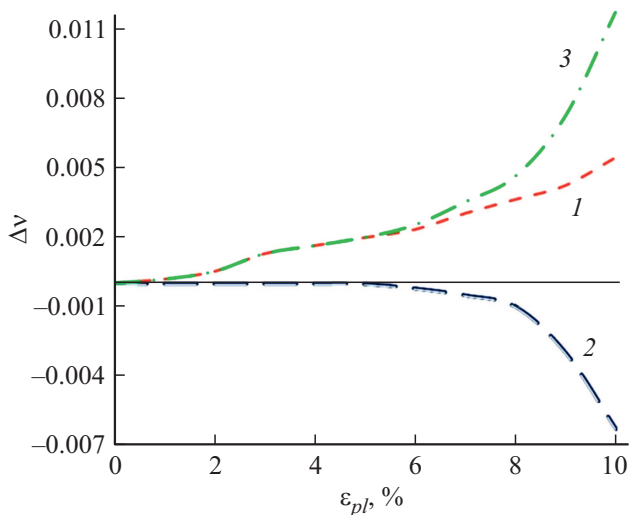


Figure 2. Change of Poisson's ratio ν (1) and its components $\nu_{\psi}^{(exp)}$ (2), ν_{Φ} (3) at early stages of plastic deformation.

and particle shape the angle Ω can be varied in a range of $[0, \pi/2]$.

Since the value of the strain-induced martensite phase yield is significantly higher, than value of austenite matrix yield [16], in the investigated model we will assume, that the rectangular particle is plastically undeformed.

Let's link the Cartesian coordinate system $Oxyz$ and associated basis $(\mathbf{e}_1, \mathbf{e}_2, \mathbf{e}_3)$ with the particle (Fig. 3, b). Concentration of particles $dn_m(\Omega, \varepsilon_{pl})$ of martensite, oriented in a range of $[\Omega, \Omega + d\Omega]$, at deformation of austenite matrix ε_{pl} for the specified geometry is defined as

$$dn_m(\Omega, \varepsilon_{pl}) = \frac{1 \mu\text{m}^3 \Phi(\varepsilon_{pl})}{1 \mu\text{m} S_m} \frac{d\Omega}{\pi/2}, \tag{6}$$

where $\Phi(\varepsilon_{pl})$ is volume fraction of martensite particles at value of plastic strain of ε_{pl} , S_m is martensite particle area, $d\Omega/(\pi/2)$ is fraction of particles, orientation of which is within a range of $[\Omega, \Omega + d\Omega]$.

During plastic deformation of austenite matrix at the boundaries of martensite particles and near them the excessive density of dislocations, that form non-homogeneous fields of internal stress, is accumulated. In general case the distribution of dislocation density (distribution of plastic strain) near the particle boundary has rather complex non-homogeneous structure, but at low deformation degrees it

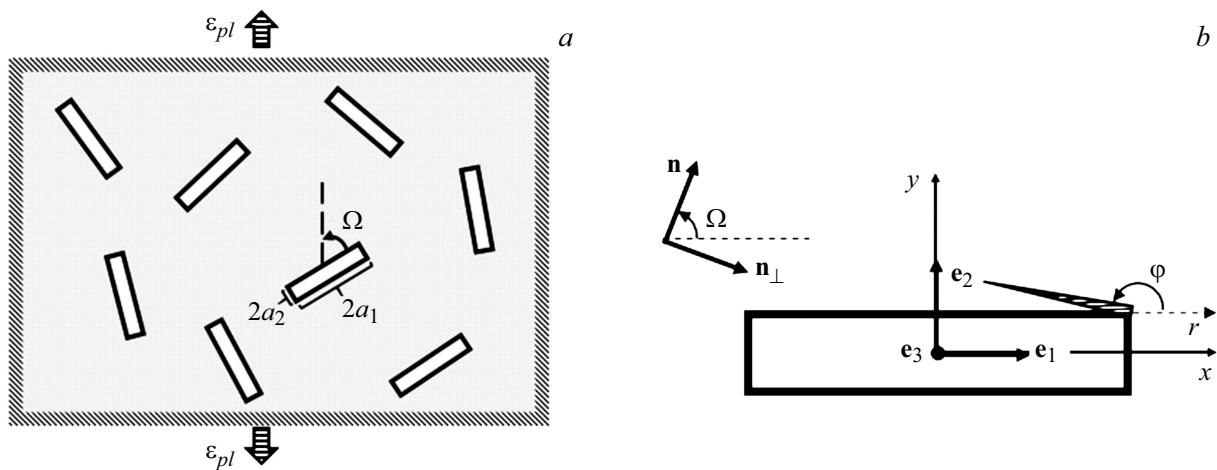


Figure 3. Scheme of austenite matrix, containing plate particles of martensite (a), and coordinate system, related to martensite particle (b).

can be conditionally assumed, that all dislocation density will be distributed along the inclusion boundary pretty much homogeneous. Despite this assumption is a rather rough approximation of actual distribution of plastic deformations near undeformed inclusion, it allows to set a simple, but aligned with plastic strain, system of internal stress sources and rather simply describe the structure of stress fields near the particle.

Density of dislocations of orientation inconsistency, induced to the particle boundary, is characterized with mismatch of plastic strain $[\epsilon_{pl}]$ at this boundary, that depends on value of ϵ_{pl} and orientation of the particle Ω :

$$[\epsilon_{pl}] = \epsilon_{pl}(\mathbf{n}(\Omega) \otimes \mathbf{n}(\Omega) - \mathbf{n}_{\perp}(\Omega) \otimes \mathbf{n}_{\perp}(\Omega)), \quad \epsilon_{pl} > 0. \quad (7)$$

For the convenience of the further calculations let's assume the stress fields, related to intrinsic homogeneous dilatation of the particle ϵ_0 , as the fields, generated with virtual dislocations, distributed along the inclusion boundary [17,18]. It should be noted, that due to presence of intrinsic dilatation of the martensite particle, significantly high compression stresses are formed in it. Tensor of density of Burgers vector \mathbf{B} [19] of dislocations at boundary of the martensite particle with normal \mathbf{N} (internal in relation to the particle) is defined as [20]:

$$\mathbf{B} = -\mathbf{N} \times ([\epsilon_{pl}] - [\epsilon_0]),$$

where $[\epsilon_0]$ is written as

$$[\epsilon_0] = \epsilon_0(\mathbf{e}_1 \otimes \mathbf{e}_1 + \mathbf{e}_2 \otimes \mathbf{e}_2), \quad \epsilon_0 > 0. \quad (8)$$

The observed distribution of virtual dislocations regarding elastic stress fields can be conveniently characterized in terms of mesodefects of simple structure: dipoles of wedge disclination with strength of \mathbf{w}_N and planar shearing mesodefects with strength of \mathbf{w}_τ [21]. Expressions for strength of mesodefects \mathbf{w}_N and \mathbf{w}_τ at the boundary with normal \mathbf{N} are written as:

$$\mathbf{w}_N = (\mathbf{e}_3 \cdot \mathbf{B} \cdot \mathbf{N})\mathbf{N}; \quad \mathbf{w}_\tau = (\mathbf{e}_3 \cdot \mathbf{B} \cdot \boldsymbol{\tau})\boldsymbol{\tau},$$

where $\boldsymbol{\tau} = \mathbf{N} \times \mathbf{e}_3$ is single vector, directed along the particle boundary. Expressions for calculation of components of tensor of elastic stress fields for the specified mesodefects are presented in Appendix [22,23].

Let's further analyze the characteristics of stable cracks, initiating near rotation-shearing mesodefects, forming during plastic strain of austenite at the boundary of martensite inclusion. It should be noted, that the approach, used in this work, is related to presentation of internal stress fields from the particle using equivalent system of virtual mesodefects and further study of initiation and propagation of microcracks and currently widely used for building the destruction models [24–27]. Let's assume, that micro-crack is formed at negative disclinations, that create large local tension stresses. For analysis of such micro-crack initiation and propagation conditions let's use the method of configuration force [28]. For plane deformation of isotropic material the expression for configuration force f , defined as a value of elastic energy, released at crack moving by a unit segment, is written as

$$f(l)_\varphi = \frac{l}{8D} (\chi(\bar{\sigma}_{\varphi\varphi})\bar{\sigma}_{\varphi\varphi}^2 + \bar{\sigma}_{r\varphi}^2), \quad (9)$$

where $D = G/[2\pi(1-\nu)]$, G is shear modulus, l is crack length, φ is polar angle, setting the orientation of the investigated crack (Fig. 3, b), $\bar{\sigma}_{\varphi\varphi}$, $\bar{\sigma}_{r\varphi}$ are average weighted total stresses near crack:

$$\bar{\sigma}_{\varphi\varphi} = \frac{2}{\pi l} \int_0^l \sigma_{\varphi\varphi}(r, \varphi) \sqrt{\frac{r}{l-r}} dr,$$

$$\bar{\sigma}_{r\varphi} = \frac{2}{\pi l} \int_0^l \sigma_{r\varphi}(r, \varphi) \sqrt{\frac{r}{l-r}} dr,$$

$$\chi(\bar{\sigma}_{\varphi\varphi}) = \begin{cases} 1, & \bar{\sigma}_{\varphi\varphi} \geq 0, \\ 0, & \bar{\sigma}_{\varphi\varphi} < 0, \end{cases}$$

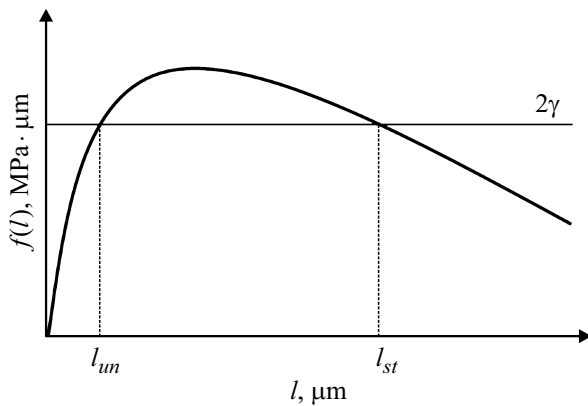


Figure 4. Scheme of dependence of configuration force f on crack length l for the investigated mesodefects at fixed φ .

where $\sigma_{\varphi\varphi}$, $\sigma_{r\varphi}$ are components of stress in polar coordinate system.

At the same time, the equivalent crack lengths l_{eq} for the specified direction φ will be defined from the relation $f(l = l_{eq}) = 2\gamma$, where γ is specific energy of a free surface. At the same time, the crack length l_{st} is called settled or stable, if it is equivalent and the condition $f'_l(l = l_{eq}) < 0$ is met, and length l_{un} is called unsettled or unstable, if it is equivalent and condition $f'_l(l = l_{eq}) > 0$ is met.

In the work [28] it was shown, that depending on type of divergence of stress function near singular stress source $\sigma \sim r^{-\alpha}$ three characteristic cases can be implemented:

1) $\alpha = 1/2$: configuration force does not depend on crack length, at $f \geq 2\gamma$ the crack initiation and propagation happen without restrictions;

2) $\alpha > 1/2$ ($f(0) \rightarrow \infty$): configuration force decreases with crack increase, crack reaches some maximum length and stops;

3) $\alpha < 1/2$ ($f(0) \rightarrow 0$): configuration force increases with crack increase, the most complicated stage of destruction is a crack initiation.

For the presented mesodefects at low r a logarithmic divergence of local stress fields is observed [21], that corresponds to the third case. At the same time, the characteristic dependence of configuration force f on crack length l for the investigated mesodefects at fixed φ is written as presented in Fig. 4.

According to Fig. 4 it follows that the configuration force $f < 2\gamma$ at $l_* < l_{un}$ and crack increase from zero to some length $l_* < l_{un}$ can not happen without additional energy boosting (as per configuration force definition). Because of that the process of crack initiation in the investigated fields of elastic stresses happens by means of other mechanisms.

For evaluation of cracks concentration let's assume, that the martensite particles already have nano-discontinuities and nano-cracks with characteristic size l_* , that appeared at the stage of the particle initiation. Let's assume, that the distribution function l_* is described with the exponential

law:

$$F(l_*) = \begin{cases} 0, & l_* < 0, \\ 1 - \exp\left(-\frac{1}{L} l_*\right), & l_* \geq 0, \end{cases}$$

where $F(l_*)$ is exponential distribution function, L is adjustable parameter.

Then, on each particle with fixed orientation and at fixed value of ε_{pl} there is a nano-discontinuity (nano-crack) with characteristic size (with length) l_* , distributed as per $F(l_*)$. At the same time, the nano-discontinuities on the particles can transform into stable crack with a length of l_{st} only if the following condition is met:

$$l_* \geq l_{un}^{\min}, \quad l_{un}^{\min} = \min_{\varphi} [l_{un}(\varphi)].$$

Therefore, only some part of nano-discontinuities will be unfold. Concentration of particles n_{cr} , oriented along direction Ω at the fixed plastic strain ε_{pl} , that have stable cracks, is defined using the following expression:

$$dn_{cr}(\Omega, \varepsilon_{pl}) = dn_m P(l_* \geq l_{un}^{\min}), \quad (10)$$

where $P(l_* \geq l_{un}^{\min})$ is possibility that nano-discontinuity length l_* will be more than l_{un}^{\min} :

$$P(l \geq l_{un}^{\min}) = F(\pm\infty) - F(l_{un}^{\min}) = \exp\left(-\frac{1}{L} l_{un}^{\min}\right).$$

At the same time, the average length of stable cracks \bar{l}_{st} is defined as

$$\bar{l}_{st} = \int_{l_{un}^{\min}}^{\infty} l_{st} P(l_* | l_* \geq l_{un}^{\min}) dl, \quad (11)$$

where $P(l_* | l_* \geq l_{un}^{\min})$ is conditional density of possibility of l_* value, l_{st} is maximum stable length, corresponding to a germ crack with a length of l_{un} . Then, the damage $d(\psi^{(th)})$, related to appearance of stable cracks on particles, orientation of which is within a range of angles $[\Omega, \Omega + d\Omega]$ (considering symmetry), is calculated as:

$$d(\psi^{(th)}) = dn_{cr} \bar{l}_{st}^3.$$

Total material damage $\psi^{(th)}$ at fixed value of plastic strain is observed by integration over the whole range of orientations of particles Ω (considering symmetry)

$$\psi^{(th)} = \int_0^{\pi/2} d\psi^{(th)}. \quad (12)$$

4. Results of numerical calculations

Numerical calculations will be performed at the following values of parameters: $G = 78\,000$ MPa, $\nu = 0.294$, $2a_1 = 1\,\mu\text{m}$, $2a_2 = 0.2\,\mu\text{m}$ — inclusion sizes, $\varepsilon_0 = 0.02$ — corresponds to increase of martensite particle volume by 2% [29]. Specific surface energy of the crack,

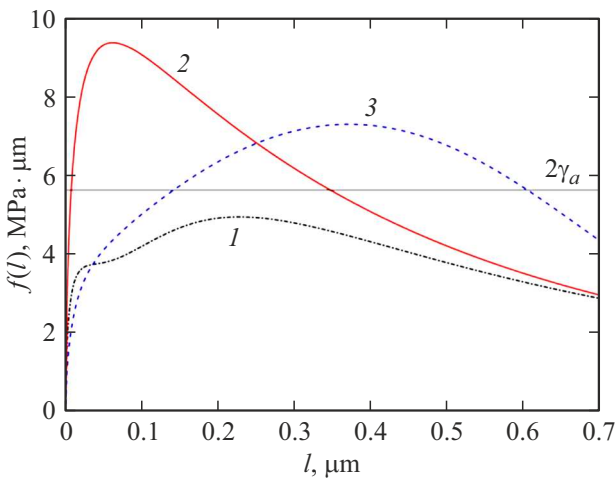


Figure 5. Characteristic dependencies of configuration force f on crack length l at its orientation angles $\varphi = 10$ (1), 60 (2) and 140° (3) and fixed values of $\varepsilon_{pl} = 0.08$ and $\Omega = \pi/3$.

formed in austenite or martensite, is evaluated as per [30] as $\gamma_a = Gb_a/10$ and $\gamma_m = Gb_m/10$ respectively, $b_a = 3.6 \cdot 10^{-4} \mu\text{m}$ — austenite lattice parameter, $b_m = 2.9 \cdot 10^{-4} \mu\text{m}$ — martensite lattice parameter. Specific surface energy of the crack, formed at non-coherent interphase boundary, γ_b is defined the same way as for high angle boundary, i.e. $\gamma_b = Gb_m/10 - Gb_m/48$. Range of plastic strain value change $\varepsilon_{pl} = 0.00 - 0.10$.

As a result of calculations, the characteristic dependencies of configuration force f on crack length l at various orientation angle values φ and fixed values of $\varepsilon_{pl} = 0.08$ and $\Omega = \pi/3$ are observed (Fig. 5). Figure 5, for instance, contains the characteristic dependencies of f on crack length l at orientation angles $\varphi = 10, 60$ and 140° , corresponding to the austenite matrix. As seen, the existence of stable crack is possible not at all orientation angles φ , but only at those, for which the condition $f_{\max}(l) > 2\gamma$

is met. For the investigated case this is the orientation angle $\varphi = 60$ and 140° . Besides, values of equivalent crack lengths for various orientation angles can be significantly different. Thus, for instance, for orientation angle $\varphi = 60^\circ$ the length of the germ crack is by an order less, than for orientation angle $\varphi = 140^\circ$, indicating that the possibility of stable crack appearance in the first direction is much higher, than in the second.

By building the similar dependencies of $f(l)$ for the whole range of angles $\varphi \in [0, 2\pi]$ the crack lengths l_u and l_{st} were defined. Figure 6 contains dependencies of these lengths l_{un} (Fig. 6, a) and l_{st} (Fig. 6, b) on orientation angle φ , observed at fixed values of $\varepsilon_{pl} = 0.08$, and $\Omega = \pi/3$. As per Fig. 6, a the germ cracks l_{un} at fixed values of $\varepsilon_{pl} = 0.08$, and $\Omega = \pi/3$ for range of angles $\varphi \in (\pi/3, 2\pi/3) \cup \{\pi\}$ take the lowest values, therefore the appearance of stable cracks, which lengths are presented in Fig. 6, b, in this range is most likely. While for angles, corresponding to martensite particle $\varphi \in (\pi, 3\pi/2)$, the germ cracks are rather large, therefore the possibility of stable cracks formation in the martensite particle is negligible.

Then, by defining the dependencies of $l_{un}(\varphi)$ and $l_{st}(\varphi)$ for all values of Ω (pitch by angle $\Delta\Omega = 10^\circ$) and all values of ε_{pl} (pitch by deformation $\Delta\varepsilon_{pl} = 0.01$), we will get the dependence of $\psi(\varepsilon_{pl})$ and, according to expression (3), $\Delta v^{(th)}$. Value of adjustable parameter L is defined from condition of minimum deviation of theoretical dependence $\Delta v_{\psi}^{(th)}(\varepsilon_{pl})$ from experimental dependence $\Delta v_{\psi}^{(exp)}(\varepsilon_{pl})$:

$$\sum \left| \Delta v_{\psi}^{(th)}(\varepsilon_{pl}) - \Delta v_{\psi}^{(exp)}(\varepsilon_{pl}) \right| \rightarrow \min. \quad (13)$$

This condition is met at $L = 174b_a \cong 0.0626 \mu\text{m}$.

Thus, to get the evaluation values of damage, (expression (12)) and change of Poisson's ratio Δv_{ψ} (expression (3)), it is necessary to set the geometry and distribution of martensite particles orientations, to define the martensite particles concentration (expression (6)), incompatibility of plastic

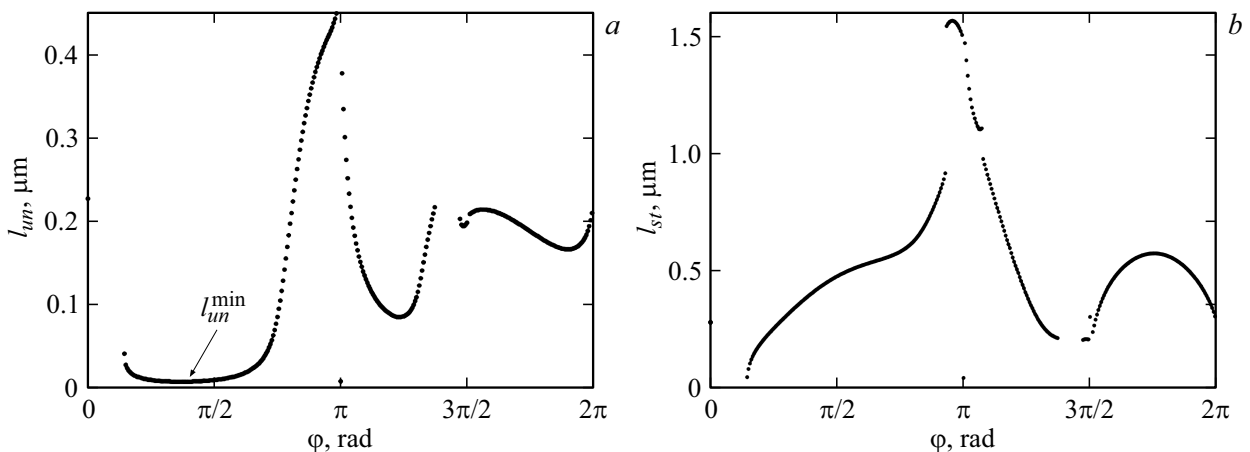


Figure 6. Dependencies of $l_{un}(\varphi)$ (a) and $l_{st}(\varphi)$ (b) at fixed values of $\varepsilon_{pl} = 0.08$, and $\Omega = \pi/3$.

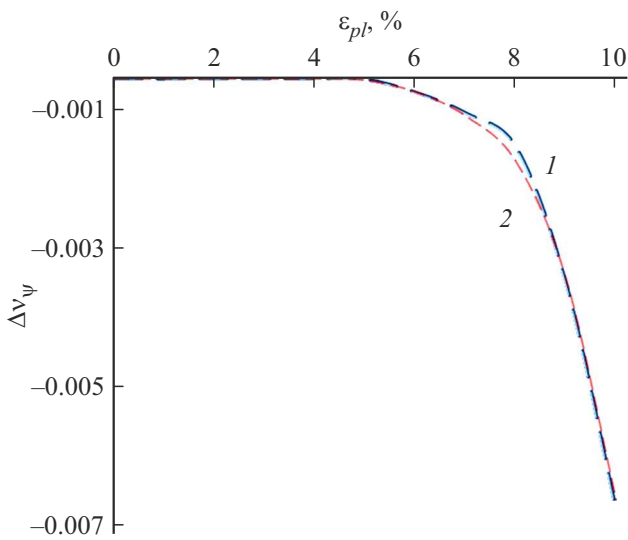


Figure 7. Comparison of $\nu_{\psi}^{(exp)}$ (1) and $\nu_{\psi}^{(th)}$ (2) at early stages of plastic deformation.

deformation (expression (7)), dilatation (expression (8)), and to calculate the elastic stress fields from martensite particles (A1–A6). Then, using configuration force method (expression (9)), define the lengths of equivalent (stable and unstable) cracks, formed in elastic stress fields from martensite particles. To determine the cracks concentration and their average length as per formulas (10) and (11) respectively, use the adjustable parameter, observed based on experimental data as per formula (13).

5. Discussion of results

Changes of the Poisson's ratio $\Delta\nu_{\psi}$ during plastic strain, observed experimentally (formula (5)) and theoretically, are presented in Fig. 7.

There is a good correlation between theoretical calculated and experimental data at strain ε_{pl} , not exceeding 10%.

The performed calculations confirmed, that damage does not impact the Poisson's ratio ν_{ψ} at strain ε_{pl} , that do not exceed 5%. With the further deformation on particles of the strain-induced martensite the new systems of rotation-shearing mesodeflects appear and create internal stress, in fields of which the micro-cracks with certain orientation form. New defects increase component ν_{ψ} in absolute value.

Conclusion

Influence of plastic deformation on Poisson's ratio, measured with acoustic method, and intensity of formation of the strain-induced martensite, which value is observed using eddy-current measurements, are studied. Experimental studies have shown, that the main influence on Poisson's ratio change is made by interrelated processes: formation

of the strain-induced martensite and accumulation of micro-damage (micro-pores, micro-cracks).

It was observed, that active change of Poisson's ratio is accompanied with active growth of the strain-induced martensite. At the later deformation stages the change intensity decreases, supposedly due to micro-damaging.

The performed modeling of formation of stable cracks, initiated near rotation-shearing mesodeflects, at the inclusion–matrix boundary has shown, that at initial stage, considering small size of cracks, contribution to Poisson's ratio increment by means of increase of the volume fraction of the strain-induced martensite prevails over contribution due to increase of number of cracks. It was observed, that density of stable micro-cracks on particles of the strain-induced martensite increases due to increase of the micro-cracks themselves and grow of existing micro-cracks. This process changes monotonous pace of Poisson's ratio value dependence on plastic strain. The performed comparison of theoretical and experimental results has shown the good agreement of curves at low deformation degrees, indicating the validity of the selected theoretical model, investigated in the work.

Funding

This study was supported financially by the Russian Science Foundation under grant №19-19-00637.

Conflict of interest

The authors declare that they have no conflict of interest.

Appendix

Expressions for calculation of components of tensors of mesodeflects elastic stress fields [22,23], defined in the right-hand Cartesian coordinate system Oxy , beginning of which coincides with the mesodeflect center, while axis Ox is directed along the mesodeflect shoulder, are written as *Planar shear mesodeflect*:

$$\sigma_{xx} = Dw_{\tau} \left[2 \left(\arctg \left[\frac{x-a}{y} \right] - \arctg \left[\frac{x+a}{y} \right] \right) + \frac{y(x+a)}{(x+a)^2 + y^2} - \frac{y(x-a)}{(x-a)^2 + y^2} \right], \quad (A1)$$

$$\sigma_{yy} = Dw_{\tau} y \left(\frac{(x-a)}{(x-a)^2 + y^2} - \frac{(x+a)}{(x+a)^2 + y^2} \right), \quad (A2)$$

$$\sigma_{xy} = Dw_{\tau} \left(\frac{y^2}{(x+a)^2 + y^2} - \frac{y^2}{(x-a)^2 + y^2} + \frac{1}{2} \ln \left[\frac{(x+a)^2 + y^2}{(x-a)^2 + y^2} \right] \right). \quad (A3)$$

Dipole of circular disclinations:

$$\sigma_{xx} = Dw_N \left(\frac{y^2}{(x+a)^2 + y^2} - \frac{y^2}{(x-a)^2 + y^2} + \frac{1}{2} \ln \left[\frac{(x+a)^2 + y^2}{(x-a)^2 + y^2} \right] \right), \quad (\text{A4})$$

$$\sigma_{yy} = Dw_N \left(\frac{y^2}{(x-a)^2 + y^2} - \frac{y^2}{(x+a)^2 + y^2} + \frac{1}{2} \ln \left[\frac{(x+a)^2 + y^2}{(x-a)^2 + y^2} \right] \right), \quad (\text{A5})$$

$$\sigma_{xy} = Dw_N \left(\frac{(x-a)y}{(x-a)^2 + y^2} - \frac{(x+a)y}{(x+a)^2 + y^2} \right), \quad (\text{A6})$$

where w_N , w_τ are values of mesodeflects strength projections w_N , w_τ on axis Ox , $2a$ is length of shearing mesodeflect or disclination dipole.

References

- [1] V.V. Mishakin, V.A. Klyushnikov, A.V. Gonchar. *Tech. Phys.*, **60** (5), 665 (2015). DOI: 10.1134/S1063784215050163
- [2] A.V. Gonchar, V.V. Mishakin, V.A. Klyushnikov, K.V. Kurashkin. *Tech. Phys.*, **62** (4), 537 (2017). DOI: 10.1134/S1063784217040089
- [3] A.V. Gonchar, V.V. Mishakin, V.A. Klyushnikov. *Int. J. Fatigue.*, **106**, 153 (2018). DOI: 10.1016/j.ijfatigue.2017.10.003
- [4] V. Mishakin, A. Gonchar, K. Kurashkin, M. Kachanov. *Int. J. Fatigue.*, **141**, 105846 (2020). DOI: 10.1016/j.ijfatigue.2020.105846
- [5] V. Mishakin, A. Gonchar, K. Kurashkin, V. Klyushnikov, M. Kachanov. *Int. J. Eng. Sci.*, **168**, 103567 (2021). DOI: 10.1016/j.jengsci.2021.103567
- [6] V.F. Terent'ev, A.G. Kolmakov, V.M. Blinov. *Deformatsiya i razrushenie materialov*, **6**, 2 (2007) (in Russian).
- [7] A.S. Vavakin, R.L. Salganik. *Mekhanika tverdogo tela*, **3**, 65 (1975) (in Russian).
- [8] R.L. Salganik. *Mekhanika tverdogo tela*, **4**, 149 (1973) (in Russian).
- [9] J.R. Bristow. *Brit. J. Appl. Phys.*, **11** (2), 81 (1960). DOI: 10.1088/0508-3443/11/2/309
- [10] M. Kachanov, I. Sevostianov. *Micromechanics of Materials, with Applications* (Springer, Cham, 2018), DOI: 10.1007/978-3-319-76204-3
- [11] E.A. Soppa, C. Kohler, E. Roos. *Mat. Sci. Eng. A*, **597**, 128 (2014). DOI: 10.1016/j.msea.2013.12.036
- [12] A.A. Zisman, V.V. Rybin. *Acta Mater.*, **44**, 403 (1996). DOI: 10.1016/1359-6454(95)00155-8
- [13] V.N. Perevezentsev, G.F. Sarafanov. *Rev. Adv. Mater. Sci.*, **30** (1), 73 (2012).
- [14] A.E. Romanov, A.L. Kolesnikova. *Progr. Mater. Sci.*, **54**, 740 (2009). DOI: 10.1016/j.pmatsci.2009.03.002
- [15] G.B. Olson, M. Cohen. *Metall. Trans. A*, **6A**, 791 (1975).
- [16] J. Post, H. Nolles, K. Datta, H.J.M. Geijselaers. *Mat. Sci. Eng. A*, **498** (1–2), 179 (2008). DOI: 10.1016/j.msea.2008.07.051
- [17] F. Kroupa, L. Lejcek. *Czech. J. Phys.*, **20**, 1063 (1970).
- [18] I.A. Ovid'ko, A.G. Sheinerman. *Rev. Adv. Mater. Sci.*, **9** (1), 17 (2005).
- [19] J.F. Nye. *Acta Met.*, **1**, 153 (1953).
- [20] R. Bullough, B.A. Bilby. *Proc. Roy. Soc.*, **B69**, 1276 (1956).
- [21] S.V. Kirikov, A.S. Pupynin, Yu.V. Svirina. *Problemy prochnosti i plastichnosti*, **83** (2), 235 (2021) (in Russian). DOI: 10.32326/1814-9146-2021-83-2-235-244
- [22] V.A. Likhachev, R.Yu. Khajrov. *Vvedenie v teoriyu disklinatsij* (LGU, L., 1975) (in Russian).
- [23] S.V. Kirikov, V.N. Perevezentsev. *Lett. Mater.*, **11** (1), 50 (2021). DOI: 10.22226/2410-3535-2021-1-50-54
- [24] M.S. Wu. *Int. J. Plasticity*, **142**, 100 (2018). DOI: 10.1016/j.ijplas.2017.10.001
- [25] G.F. Sarafanov, V.N. Perevezentsev. *Deformatsiya i razrusheniya materialov*, **2**, 2 (2016) (in Russian).
- [26] M.Yu. Gutkin, I.A. Ovid'ko, N.V. Skiba. *Phys. Solid State*, **49**, 261 (2007). DOI: 10.1134/S1063783407020138
- [27] M.Yu. Gutkin, I.A. Ovid'ko. *Phil. Mag. Lett.*, **84** (10), 655 (2004). DOI: 10.1080/09500830512331329123
- [28] V.L. Indenbom. *FTT*, **3**, 2071 (1961) (in Russian).
- [29] V.G. Chashchina, M.P. Kashchenko. *Ekspperimental'nye osnovaniya dinamicheskoy teorii martensitnykh prevrashchenij* (Izd-vo Ural. un-ta, Ekaterinburg, 2020) (in Russian).
- [30] J. Friedel. *Dislocations* (Pergamon Press, Oxford, 1964)